Supporting Information

A Fluorinated Chiral Liquid with Thermal Robustness for Inducing Circularly Polarized Luminescence

Zibing Xiao, [ab] Runjia Wang, [ab] Li Zhang, [*a] and Minghua Liu [*ab]

a. Beijing National Laboratory for Molecular Science (BNLMS), CAS Key Laboratory of Colloid, Interface and Chemical Thermodynamics, Institute of Chemistry, Chinese Academy of Sciences, Beijing, China.

b. University of Chinese Academy of Sciences, Beijing, China.

*Corresponding authors: Li Zhang, Minghua Liu

E-mail: zhangli@iccas.ac.cn, liumh@iccas.ac.cn

Contents

Materials

All chemicals were purchased commercially and used without further purification. Pentadecafluorooctanoyl chloride ($C_7F_{15}COCl$, 97 %) and coumarin 7 (98 %) were purchased from Aladdin. L-&D-Glutamic dimethyl ester hydrochloride (L-&D-GluDME·HCl, 98 %) were purchased from Innochem. Triethylamine (Et3N, 99 %) was purchased from J&K. Hydrochloric acid (HCl, 36-38 % aqueous solution) was purchased from Xilong Scientific. Rhodamine 6G (R6G, >95 %) was purchased from Acros. Carbazole (97 %) and Chloroform-d ($CDCl_3$, 99.8%, TMS, 0.03%) were purchased from Energy Chemical. Dichloromethane (CH_2Cl_2, AR, 99.5 %), tetrahydrofuran (THF, AR, 99.7 %), ethyl acetate (EA, GR, 99.8%) and N, N-Dimethylformamide (DMF, AR, 99.7 %) was purchased from Concord. The water used in all experiments was of Millipore Milli-Q grade (18.2 MΩ cm).

Synthesis and preparation

Synthesis of L-C_7FGM

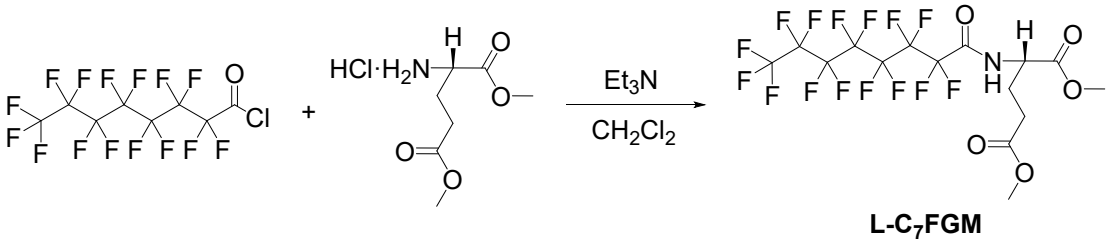

Scheme S1 Synthetic routes to **L-C_7FGM**

L-GluDME·HCl (2.465 g, 12.5 mmol) was dissolved in 50 mL CH_2Cl_2 in a 250 mL round flask. Triethylamine (3.177 g, 31.2 mmol) was added and the mixture was stirred at room temperature for 20 mins. $C_7F_{15}COCl$ (5.405 g, 12.5 mmol) and 20 mL CH_2Cl_2 were mixed up to prepare a $C_7F_{15}COCl$ solution. The $C_7F_{15}COCl$ solution was dripped into the round flask costing 30 minutes and producing a white smoke. If the drip process was stopped, the smoke would disappear in few minutes during the stirring. The mixture was stirred at room temperature overnight. After the reaction had been finished, the organic solvent and low boiling point impurities were removed by using rotary evaporator and 50 mL CH_2Cl_2 was added again to dissolve. The reaction mixture was washed with 50mL HCl (Diluted to 3 %) aqueous solution for three times and washed with 50 mL pure water for three times. The organic phase was collected and organic solvents were evaporated and 5.315 g target products were obtained by above series operations with a yield of 74.5 %. The **L-C_7FGM** is white to pale yellow waxy solid at room temperature and will easily melt to liquid under a temperature higher than 37 ^oC.

^{1}H NMR (400 MHz, Chloroform-d, 298 K): δ 7.53 (d, *J* = 6.3 Hz, 1H), 4.65 (td, *J* = 7.5, 5.0 Hz,

1H), 3.80 (s, 3H), 3.70 (s, 3H), 2.55 – 2.34 (m, 2H), 2.34 – 2.07 (m, 2H). **Figure S27**

^{13}C NMR (101 MHz, Chloroform-d, 298K, experiment with proton decoupling) δ 173.4, 170.6, 157.6, 118.5, 115.7, 110.5, 108.9, 107.8, 106.2, 52.9, 52.5, 52.0, 29.7, 26.3. **Figure S28**

^{19}F NMR (565 MHz, Chloroform-d, 298K) δ -80.9, -119.9, -121.6, -122.1, -122.5, -122.8, -126.2. **Figure S29**

MALDI-FITCR-MS: calc: $C_{15}H_{12}F_{15}NO_5$ = 571.24, found: 594.04 $(M + Na)^+$, 610.01 $(M + K)^+$. **Figure S31**

Synthesis of D-C$_7$FGM

D-C$_7$FGM was synthesized as the above-mentioned procedures of **L-C$_7$FGM** except D-GluDME·HCl was used instead of L-GluDME·HCl.

^{1}H NMR (400 MHz, Chloroform-d, 298K) δ 7.51 (d, *J* = 7.4 Hz, 1H), 4.65 (td, *J* = 7.2, 5.0 Hz, 1H), 3.80 (s, 3H), 3.70 (s, 3H), 2.54 – 2.35 (m, 2H), 2.35 – 2.07 (m, 2H). **Figure S30**

Preparation of the dyes@C$_7$FGM samples

The dyes used in this article including rhodamine 6G, coumarin 7, carbazole. One kind of Dyes (5 mg) and **L-/D-C$_7$FGM** (495 mg) were dissolved in 200 uL CH_2Cl_2 in a 2 mL phial. The phial was put in an air blast drying oven under 80 ^oC to evaporate all the CH_2Cl_2. The sample of 1% **dyes@C$_7$FGM** would be prepared until the mass of phial maintained at constant weight.

Characterization

UV-Vis, CD, LD, FL and CPL spectra

UV-Vis absorption spectra were measured with a Hitachi U-3900 Spectrophotometer. The circular dichroism (CD) and variable temperature CD spectra were recorded in a JASCO J-815 spectropolarimeter attached a variable temperature attachment if needed. The linear dichroism (LD) spectra were recorded in a JASCO J-1500 spectropolarimeter. The fluorescence emission and variable temperature fluorescence (FL) emission spectra were operated on a Hitachi F4600 instrument with excitation voltage of 400 V. The instrument would attach a variable temperature attachment for variable temperature measurements. The circularly polarized luminescence (CPL) and variable temperature CPL spectra were performed on a JASCO CPL-300 spectrometer attached a variable temperature attachment if needed. All the UV-Vis, CD, FL and CPL spectra of the system involving **C$_7$FGM** were measured by using the pair of 0.1 mm light path quartz plates and above-mentioned spectra of the system without **C$_7$FGM** were measured by using the 10 mm light path quartz cells. All the variable temperature spectra were measured *in situ*.

Fluorescence lifetime

Fluorescence lifetime data were recorded with an Edinburgh FLS-980 photospectrometer.

NMR and mass spectra

The ^{1}H and ^{13}C NMR spectra were recorded on a Bruker AVANCE HD 400 machine and the ^{13}C NMR was experimented with proton decoupling. The ^{19}F NMR spectra were recorded on a Bruker AVANCE HD 600 machine. Mass spectra were obtained using a Bruker solariX Maldi-FTICR-MS instrument.

SEM

Scanning electron microscopy (SEM) was carried out on a Hitachi S-4800 FE-SEM microscope under an accelerating voltage of 10 or 5 kV. The liquid C_7FGM was dripped on the silicon wafers and cooled to solidify. A fine tip was used to destroy the solidified smooth surface making the inside structure to be exposed. Before SEM measurements, the solid samples on silicon wafers were coated with a thin layer of Pt to increase the contrast.

XRD

Variable temperature X-ray diffraction (XRD) patterns were achieved on a Malvern Panalytical Empyrean X-ray diffractometer with CuKa radiation (λ = 1.5406 Å), which were operated at a voltage of 40 kV and a current of 40 mA. Solid samples were cast on aluminum oxide substrates and temperature was controlled by the variable temperature program of X-ray diffractometer in which the solid sample would melt and liquid would be measured *in situ*.

ATR-FTIR

Attenuated total reflection Fourier transform infrared (ATR-FTIR) spectra were recorded by a Bruker TENSOR27 spectrophotometer with an ATR attachment. The solid sample was coated on the plate of ATR and measured at first. Then the solid was heated and illuminated *in situ* by a handheld infrared light for over 5 minutes to ensure that the solid sample melted and could keep liquid statement during the subsequent measurement.

DSC and TGA

Differential scanning calorimetry (DSC) measurements were performed using a METTER TOLEDO DSC3. Nitrogen purge (flow rate: 50 mL/min) was performed during all the experiments. In the DSC measurements showed **Fig 2a**, the heating rate was 10 K/min. In the DSC measurement showed **Fig 2b**, the sample was heated from 303K to 353K in 5 minutes (heating rate: 10 K/min) and the temperature was kept for 1 hour. Thermal gravimetric analysis (TGA) measurements were

performed using a METTER TOLEDO TGA2. Nitrogen purge (flow rate: 50 mL/min) was performed during all the experiments and the heating rate was 10 K/min for all the experiments.

Rheology measurements

Rheology measurements were carried on an Anton Paar MCR 502 stress-controlled rheometer with a 50mm smoothed parallel-plate geometry and the temperature was controlled by the variable temperature program of rheometer. Dynamic frequency sweep measurements were conducted in the linear viscoelastic region (shear strain γ = 1 %). The complex viscosity values showed in **Fig 2d** were calculated by using **Equation1** in which storage modulus (G') and loss modulus (G") were measured by rheology measurements.

$$Complex\ viscosity = \frac{\sqrt{G'^2 + G''^2}}{\omega}\ [Pa \cdot s] \quad \textbf{Equation 1}$$

Polarizing optical microscope

The polarizing optical photos were taken by the polarizing optical mode of Olympus IX 83 inverted fluorescence microscope.

Methods of MD and DFT simulation

Molecular dynamics simulations of optimal arrangement of **L-C$_7$FGM** were conducted utilizing the GROMACS software version 2020.6[1] within a cubic box of dimensions 3.7 nm x 4.5 nm x 4.8 nm, employing the General Amber Force Field (GAFF). The initial coordinates comprised 30 pre-arranged molecules, which were inferred from X-ray diffraction (XRD) data. Subsequently, an additional 48 molecules were randomly introduced into the box using GROMACS. The topology files for the molecules were computed using the Gaussian 16 program[2], with the DFT/B3LYP/6-311G* basis set[3], ultimately generated by Multiwfn[4-6]. The generated input coordinates for all systems were then energy minimized using the steepest descent algorithm. To explore the causes of the varying optical signals emitted by dye molecules in solution due to temperature changes, the temperature was elevated and maintained at 273K, 313K, and 353K for 20 ns each, using the Leap-Frog algorithm. Structural differences among the molecules were subsequently observed.

To elucidate and clarify the conformation of dye molecules in this solvent, we filled a box of 5 nm x 5 nm x 5 nm with 200 solvent molecules. The initial conformation of the molecules is still derived from the DFT method, and the functional and basis set are B3LYP/6-311G*. After equilibrating the system for 20 ns at 313 K, we and added one dye molecule each and further simulated for 20 ns, obtaining the average conformation of dye molecules ranging from 15-20 ns. The TD-DFT task was calculated using ORCA[7] software with this conformation, and the corresponding molecule's ECD spectra were plotted using Multiwfn software. The PBE0/def2-TZVP (-f) group was used for coumarin 7 molecules, while the CAM-B3LYP/def2-TZVP (-f) group was used for R6G molecules.

Supplementary figures

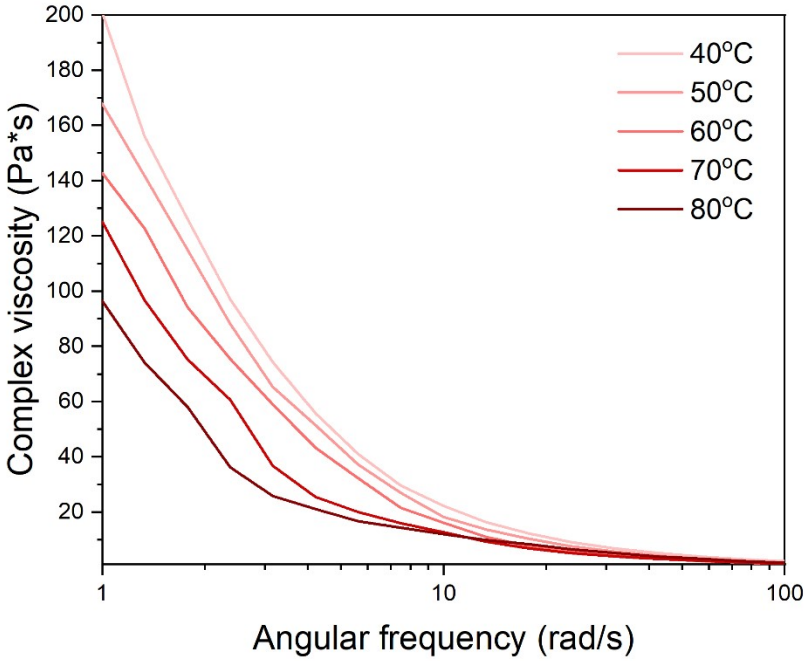

Figure S1 Variable temperature complex viscosity of L-C_7FGM

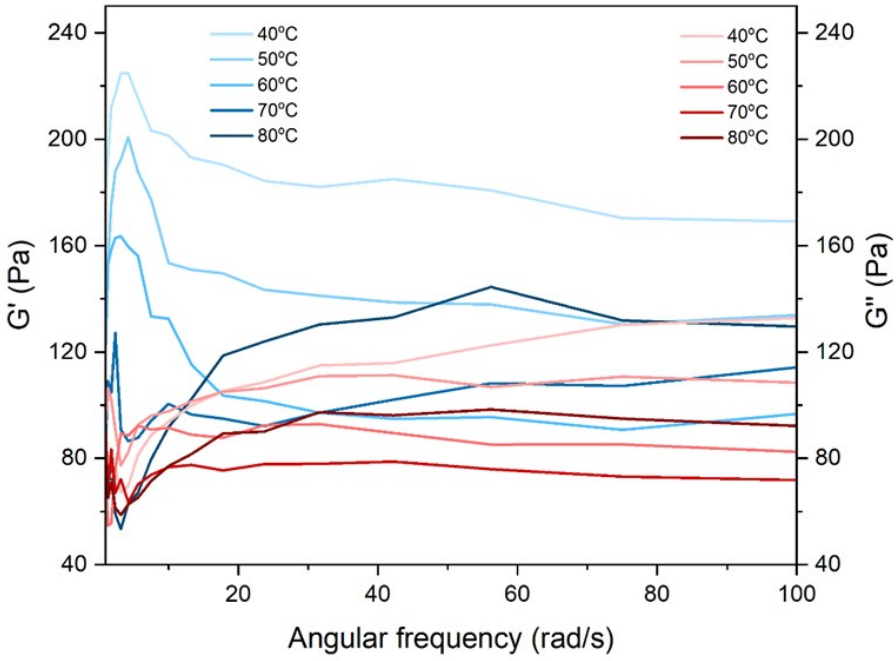

Figure S2 Storage modulus (G', blue series lines) and loss modulus (G", red series lines) of **L-C_7FGM**

at Variable temperature**.**

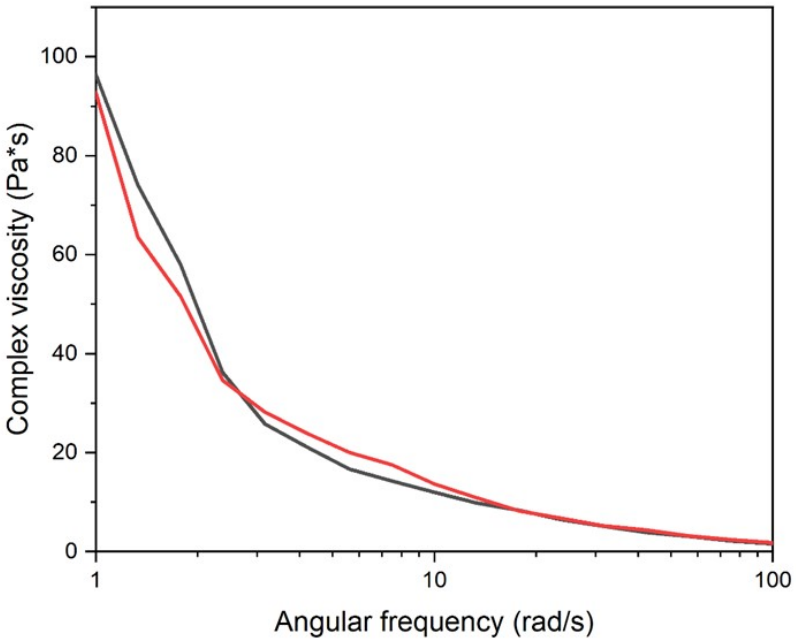

Figure S3 Complex viscosity of **L-C$_7$FGM** when it first reached 80 °C (black line) and after maintained the temperature for 1 hour (red line).

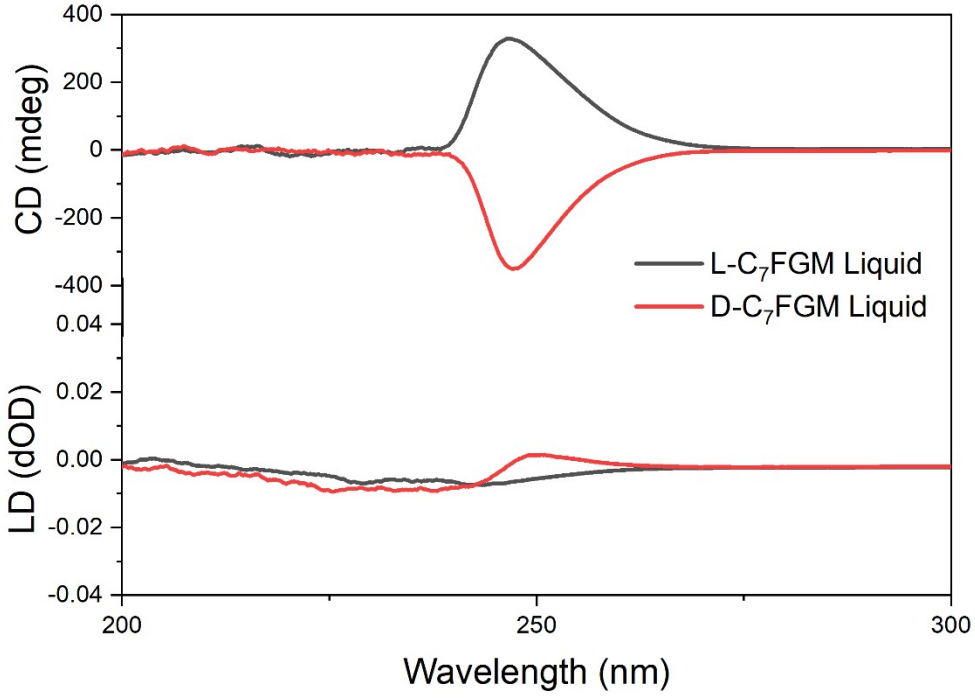

Figure S4 CD and LD spectra of liquid **L-/D-C$_7$FGM**. Only very slight LD signals were observed.

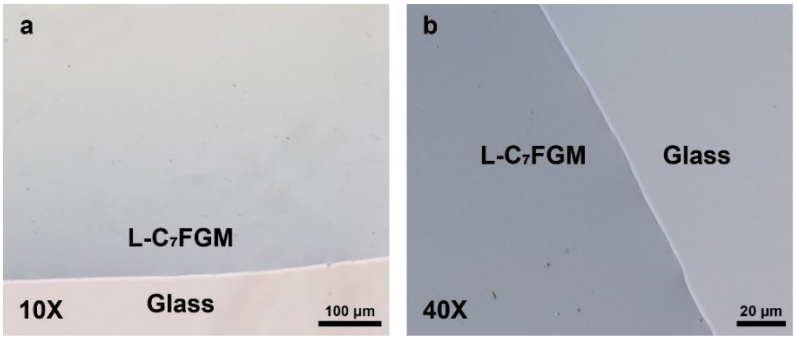

Figure S5 The 10x (a) and 40x (b) magnification photos of **L-C$_7$FGM** liquid taken by the polarizing optical microscope. The homochromous and homogeneous images confirmed the isotropy of **L-C$_7$FGM** liquid.

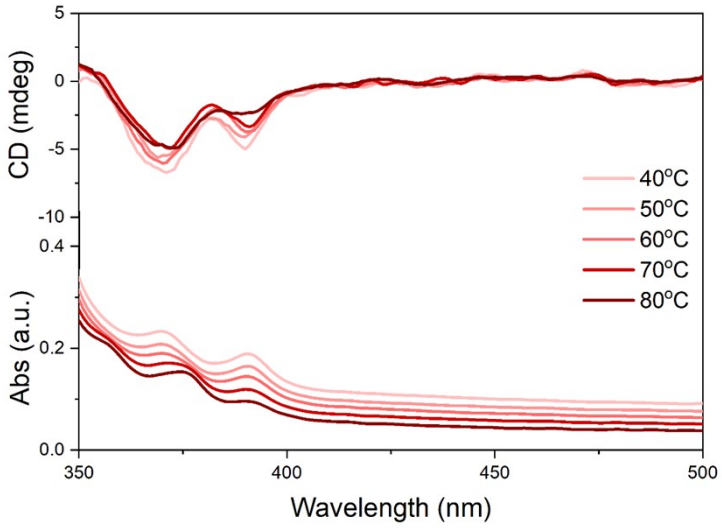

Figure S6 Variable temperature CD spectra of 1% **carbazole@ L-C$_7$FGM liquid**.

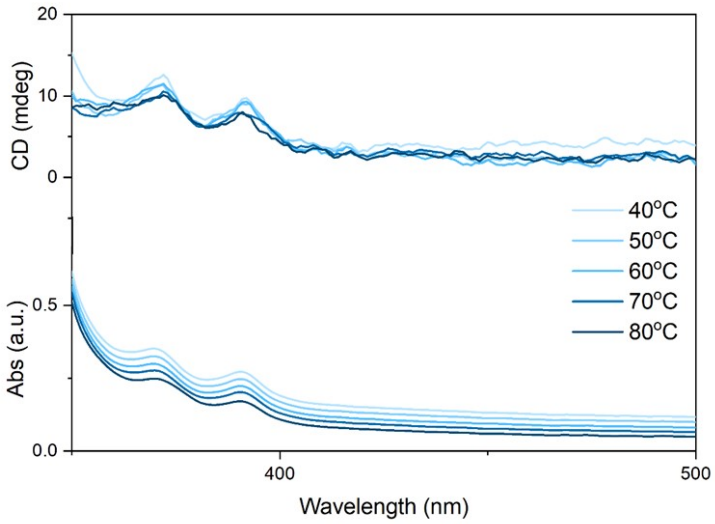

Figure S7 Variable temperature CD spectra of 1% **carbazole@ D-C$_7$FGM liquid**.

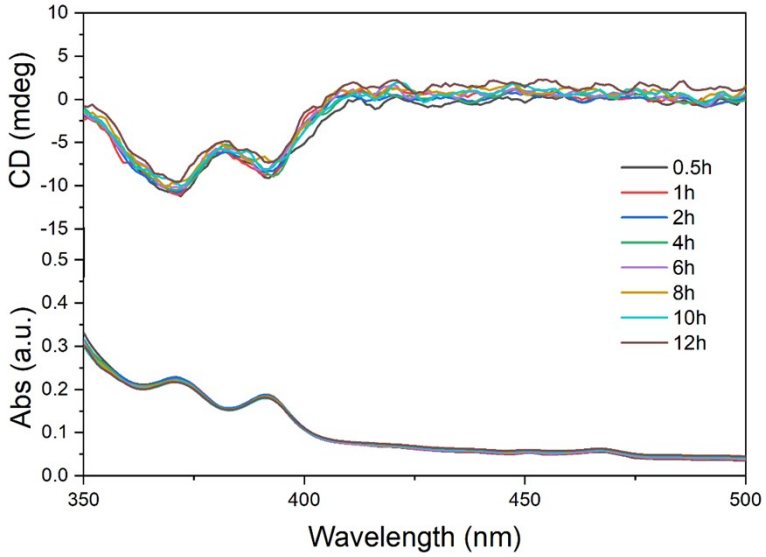

Figure S8 CD spectra for different maintaining time at 80 °C of 1% **carbazole@ L-C_7FGM**.

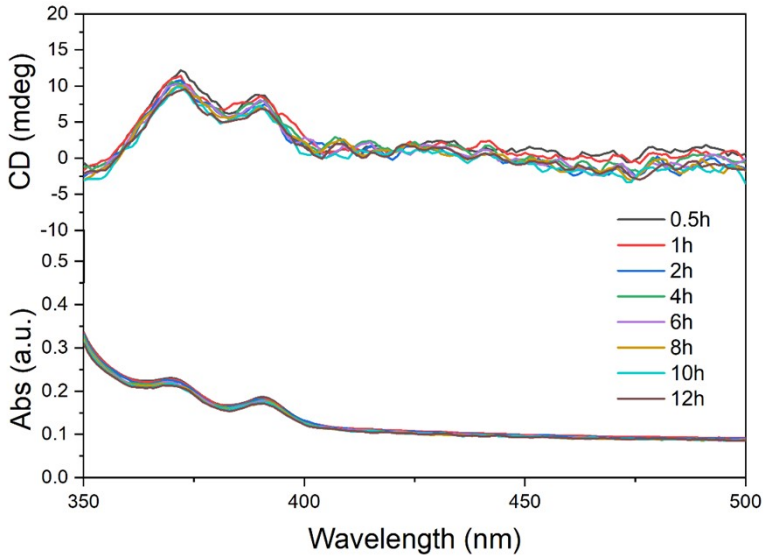

Figure S9 CD spectra for different maintaining time at 80 °C of 1% **carbazole@ D-C_7FGM**.

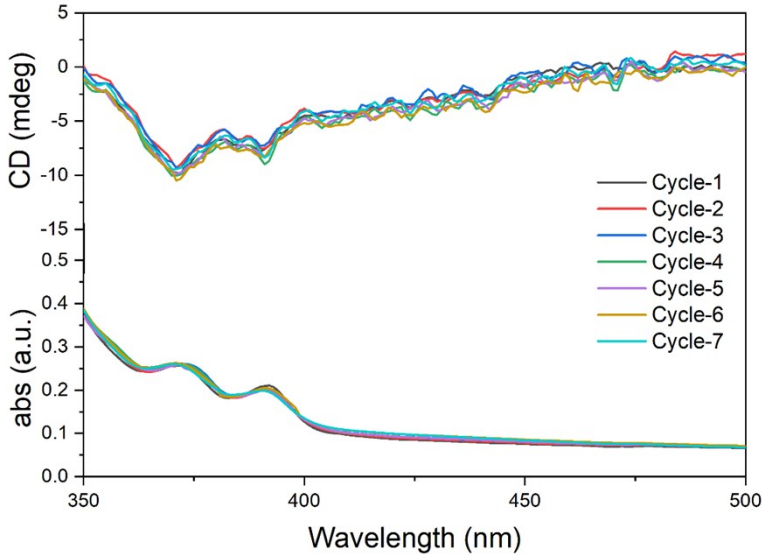

Figure S10 CD spectra of 1% **carbazole@ L-C_7FGM** after every cooling-heating cycle (measured at 80 °C).

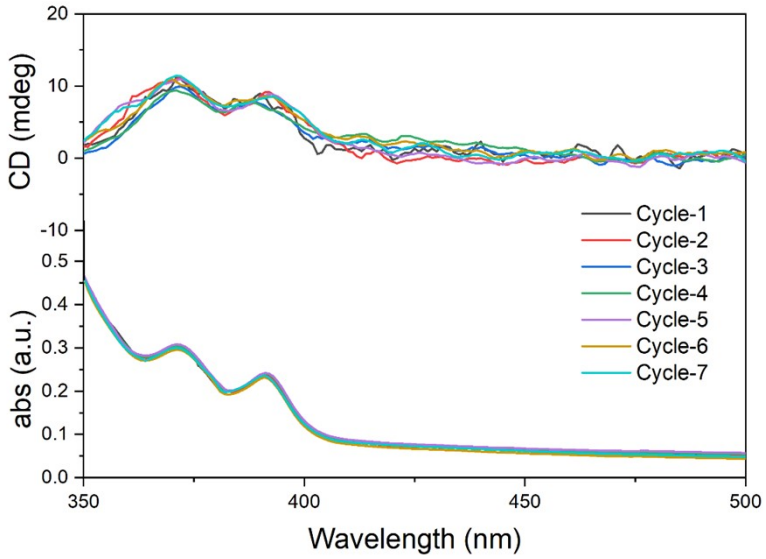

Figure S11 CD spectra of 1% **carbazole@ D-C_7FGM** after every cooling-heating cycle (measured at 80 °C).

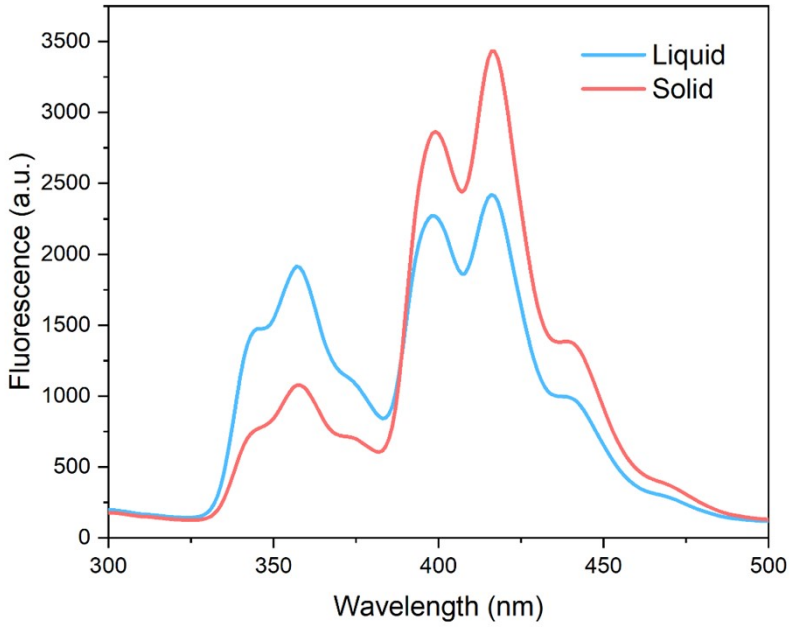

Figure S12 Fluorescence emission spectra of **1% carbazole@ L-C$_7$FGM** system (Ex = 270 nm) at liquid and solid phase. The peaks before 390 nm diminished and the peaks after 390 nm enhanced.

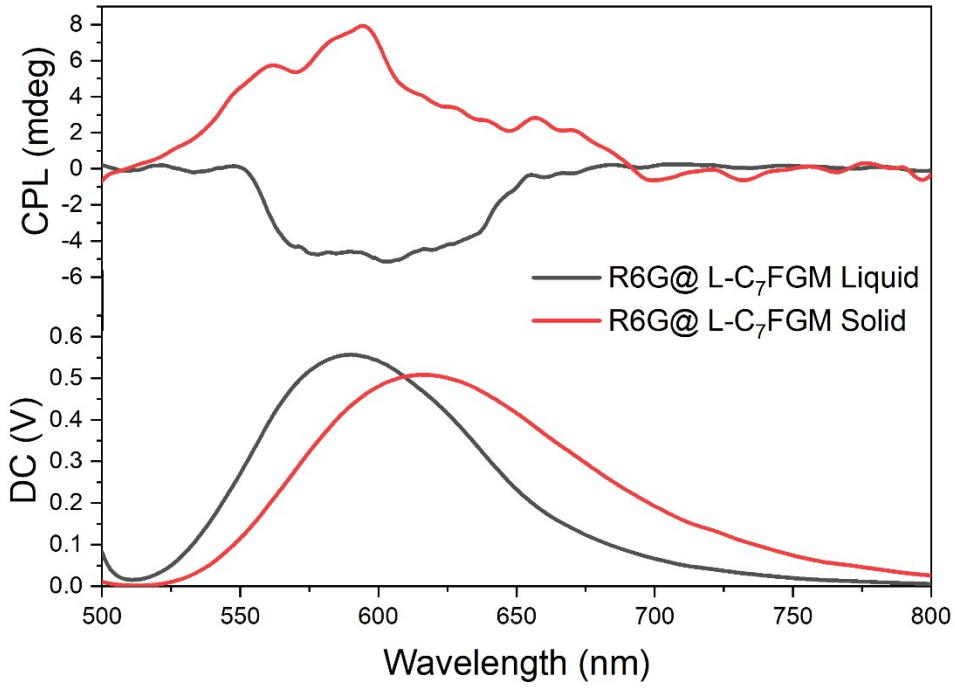

Figure S13 CPL spectra of **1% R6G@ L-C$_7$FGM** (Ex = 460 nm) at liquid and solid phase.

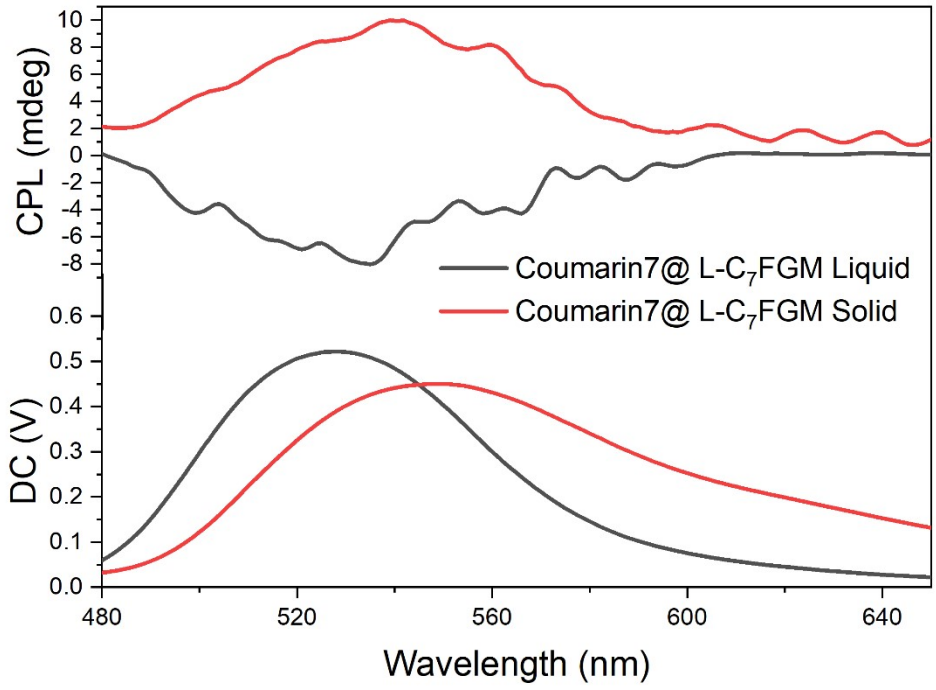

Figure S14 CPL spectra of **1% Coumarin7@ L-C$_7$FGM** (Ex = 430 nm) at liquid and solid phase.

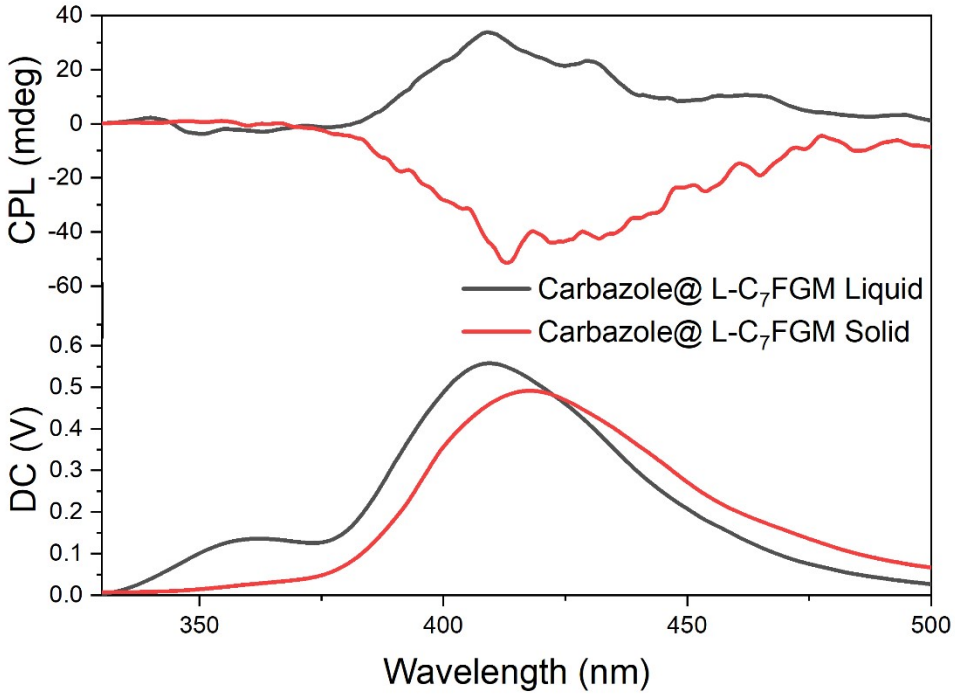

Figure S15 CPL spectra of **1% Carbazole@ L-C$_7$FGM** (Ex = 270 nm) at liquid and solid phase.

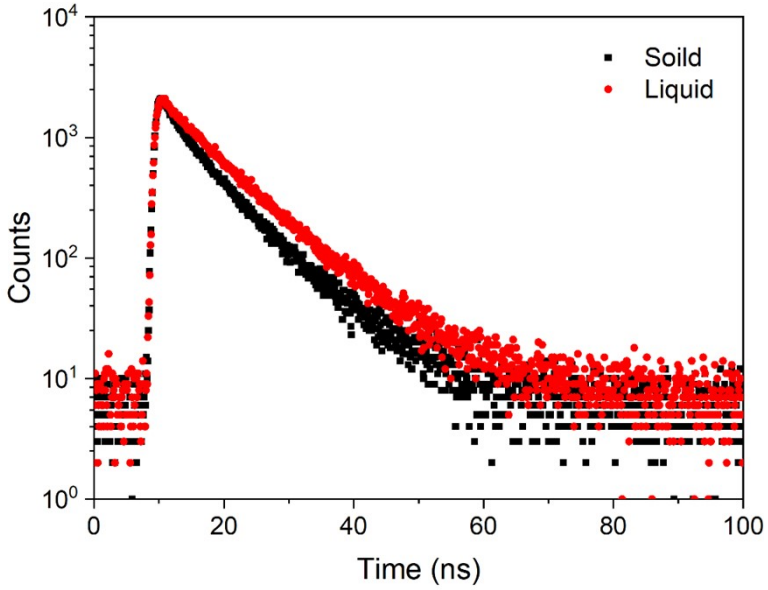

Figure S16 Fluorescence lifetime of **1% carbazole@ L-C_7FGM** system (Ex = 270 nm) at liquid (8.9 ns) and solid (7.1 ns) phase, which indicate that the carbazole emits fluorescence in **L-C_7FGM**.

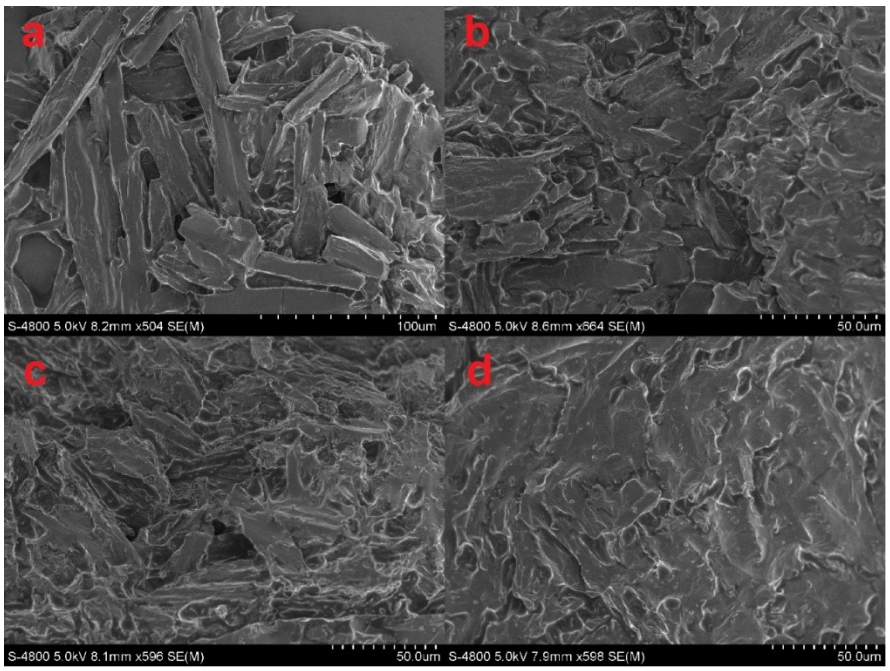

Figure S17 SEM pictures of **a) pure L-C_7FGM, b) 1% R6G@ L-C_7FGM, c) 1% coumarin7@ L-C_7FGM and d) 1% carbazole@ L-C_7FGM.** Those similar structure confirmed that the doped dyes did not separate from solid **L-C_7FGM.**

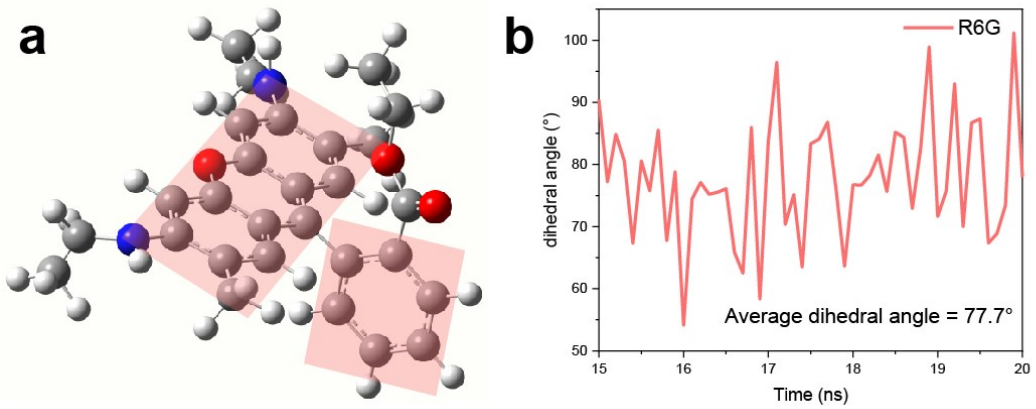

Figure S18 (a) Average conformation of R6G in L-C_7FGM in which the rotation of single bond between two marked aromatic rings is limited. (b) The values of dihedral angle of two rings in last 5 ns in MD simulation.

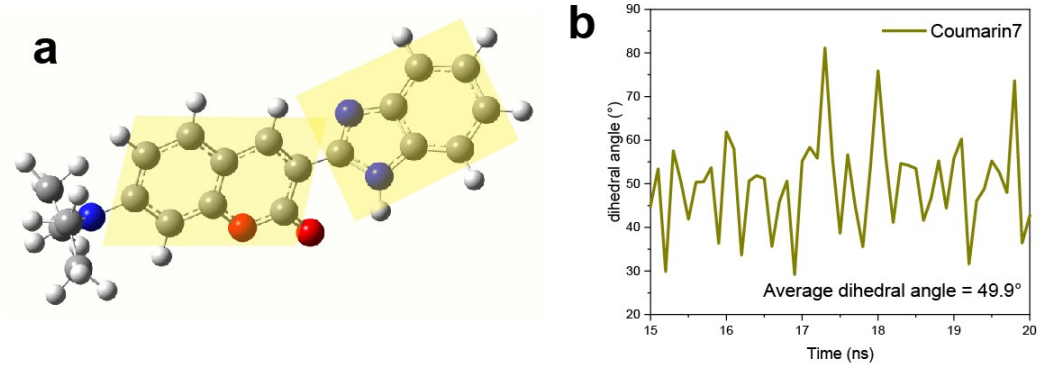

Figure S19 (a) Average conformation of coumarin7 in L-C_7FGM in which the rotation of single bond between two marked aromatic rings is limited. (b) The values of dihedral angle of two rings in last 5 ns in MD simulation.

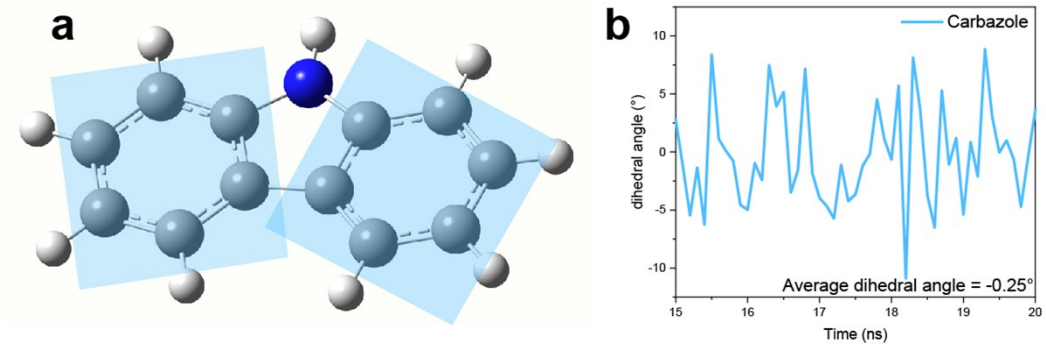

Figure S20 (a) Average conformation of carbazole in L-C_7FGM in which the carbazole is rigidity and planar. (b) The values of dihedral angle of marked two rings in last 5 ns in MD simulation.

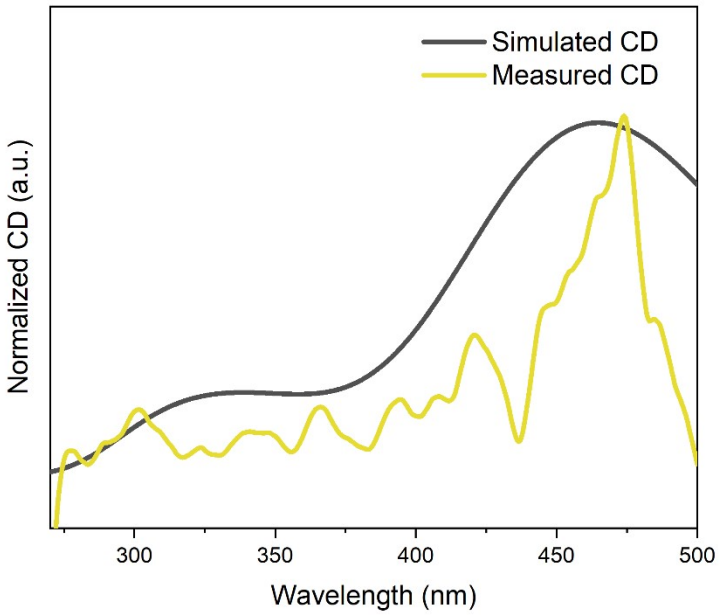

Figure S21 The simulated CD by DFT and measured CD of coumarin7 in **L-C$_7$FGM**.

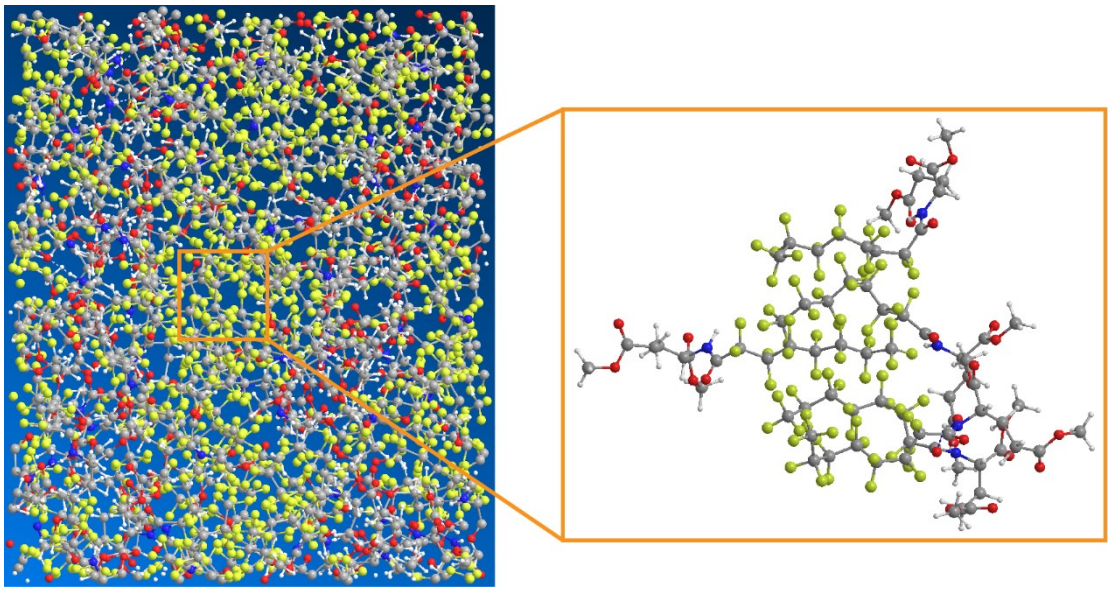

Figure S22 Molecular dynamic simulation results of 78 **L-C$_7$FGM** molecules at 273K. Five of the molecules in a representative arrangement were zoomed and displayed at right box.

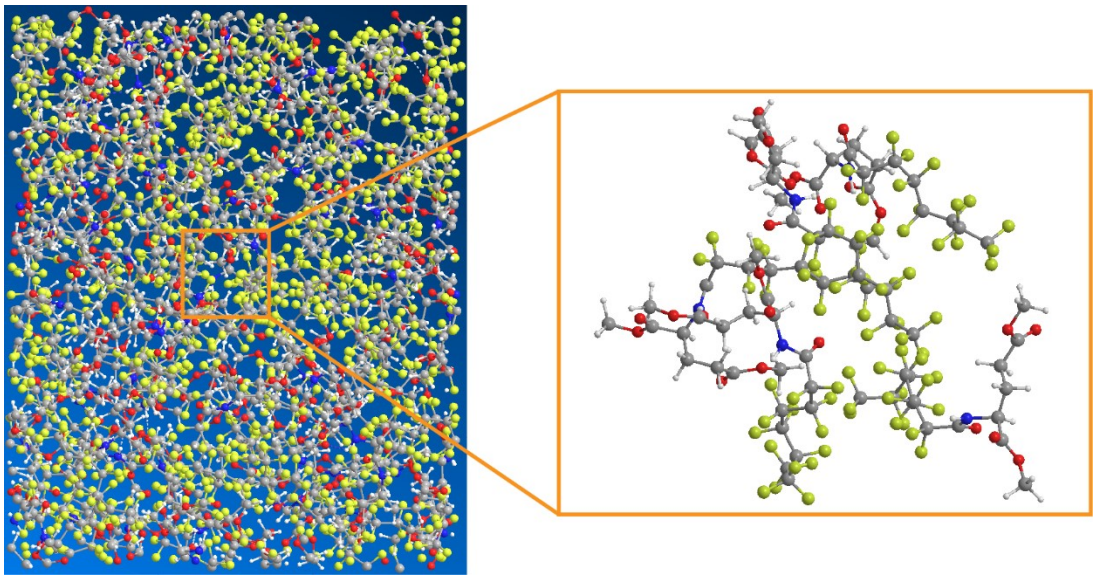

Figure S23 Molecular dynamic simulation results of 78 **L-C$_7$FGM** molecules at 313K. Five of the molecules in a representative arrangement were zoomed and displayed at right box.

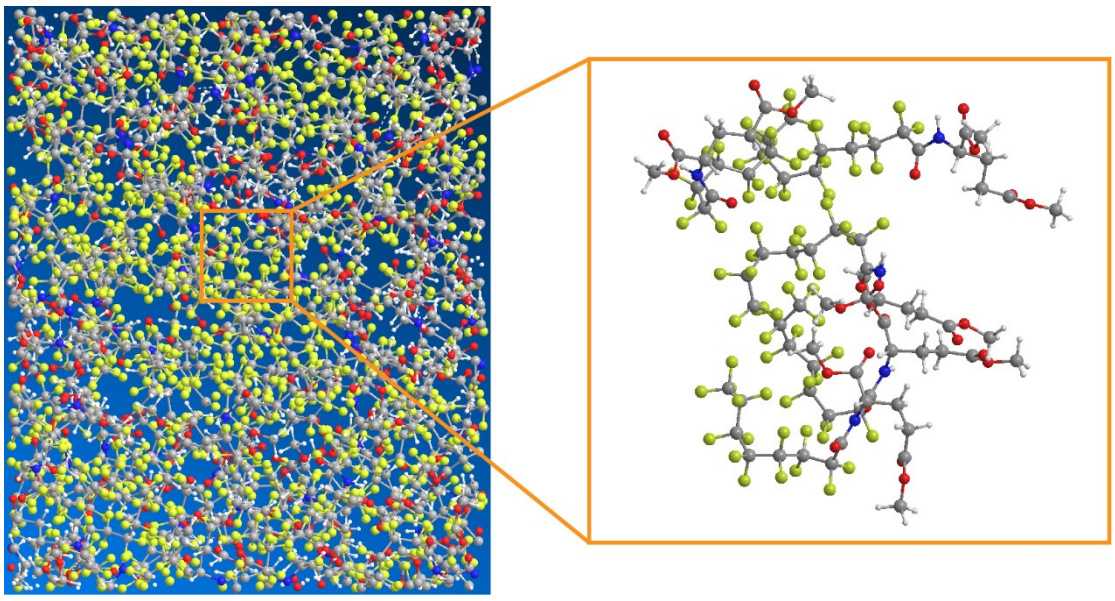

Figure S24 Molecular dynamic simulation results of 78 **L-C$_7$FGM** molecules at 353K. Five of the molecules in a representative arrangement were zoomed and displayed at right box.

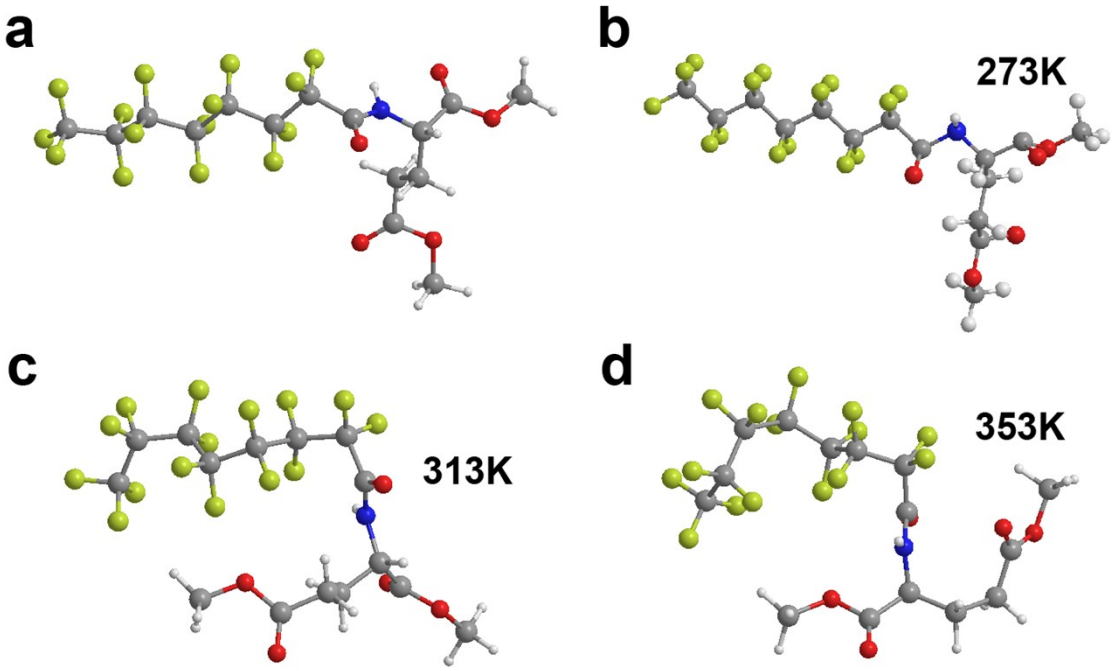

Figure S25 a) The single molecule conformation simulated by density functional theory (DFT) in vacuo. b), c) and d) A representative single molecule conformation chosen from the MD simulation results at 273K, 313K and 353K, respectively.

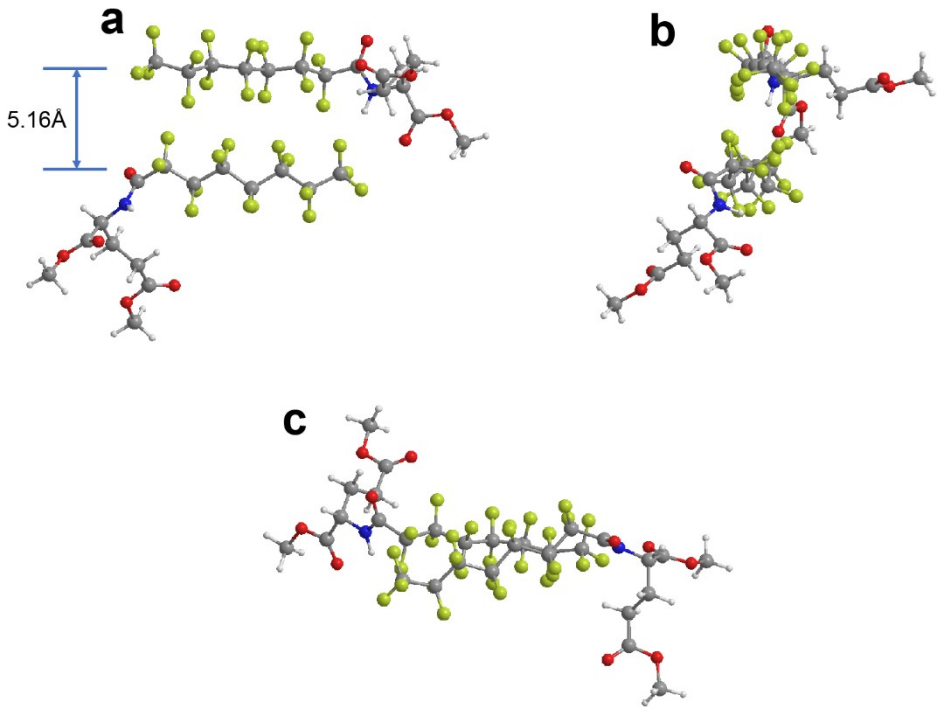

Figure S26 The DFT simulation results of two molecules conformation in different angles of view.

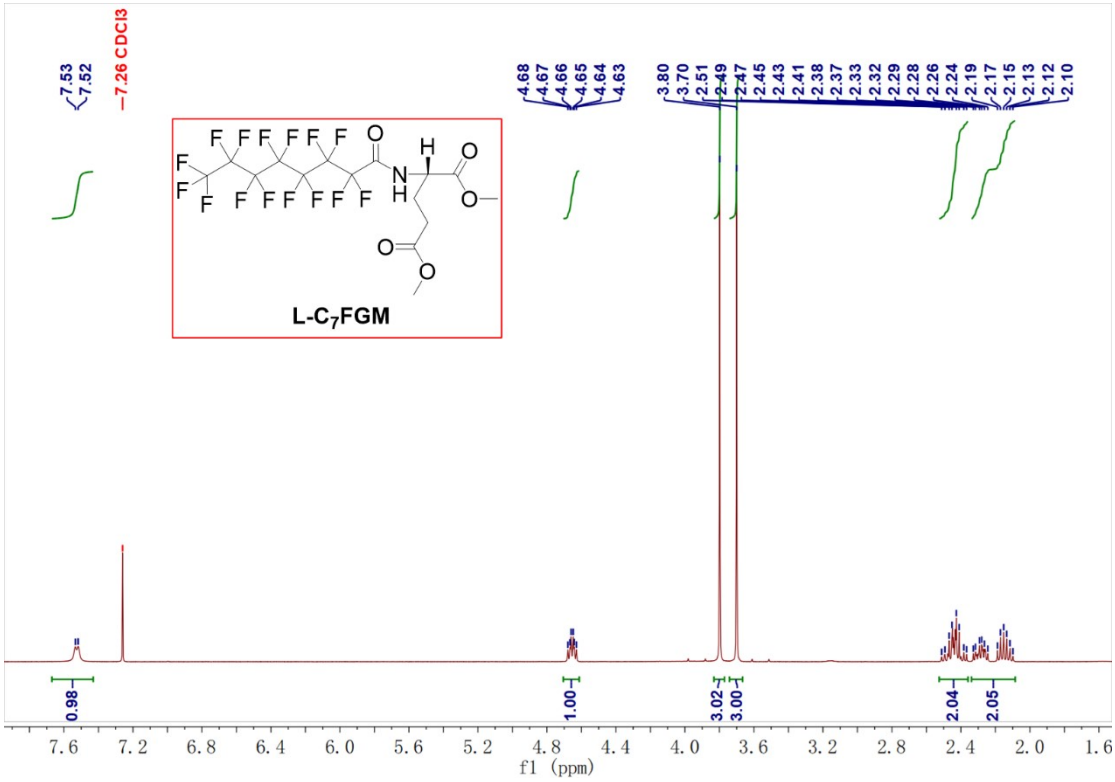

Figure S27 ^{1}H NMR spectrum of **L-C$_7$FGM**. The peak at 7.26 ppm is attributed to the solvent peak of Chloroform-d.

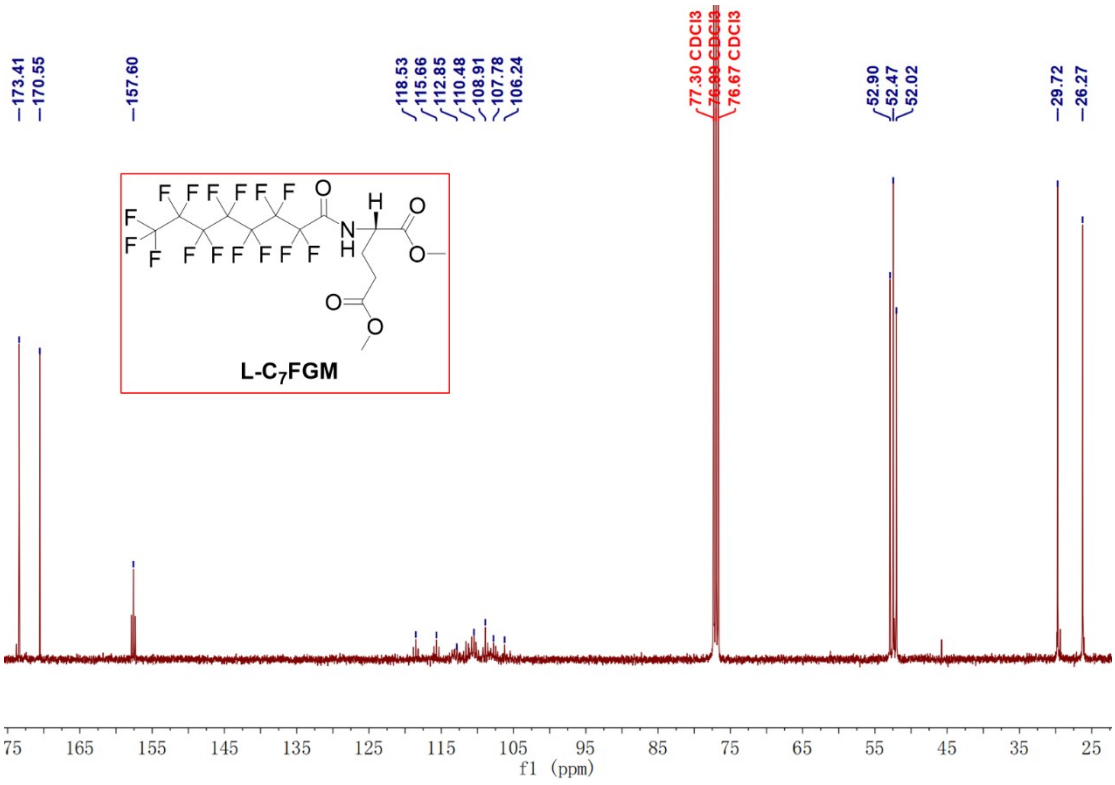

Figure S28 ^{13}C NMR spectrum of **L-C$_7$FGM**. The ^{13}C NMR was experimented with proton decoupling. The triple peaks at 157.6 ppm and the multiple peaks at the range of 106-119 ppm are split caused by the coupling of adjacent fluorine atoms to carbon atoms. The peaks at the range of 76.7-77.3 ppm are

attributed to the solvent peak of Chloroform-d.

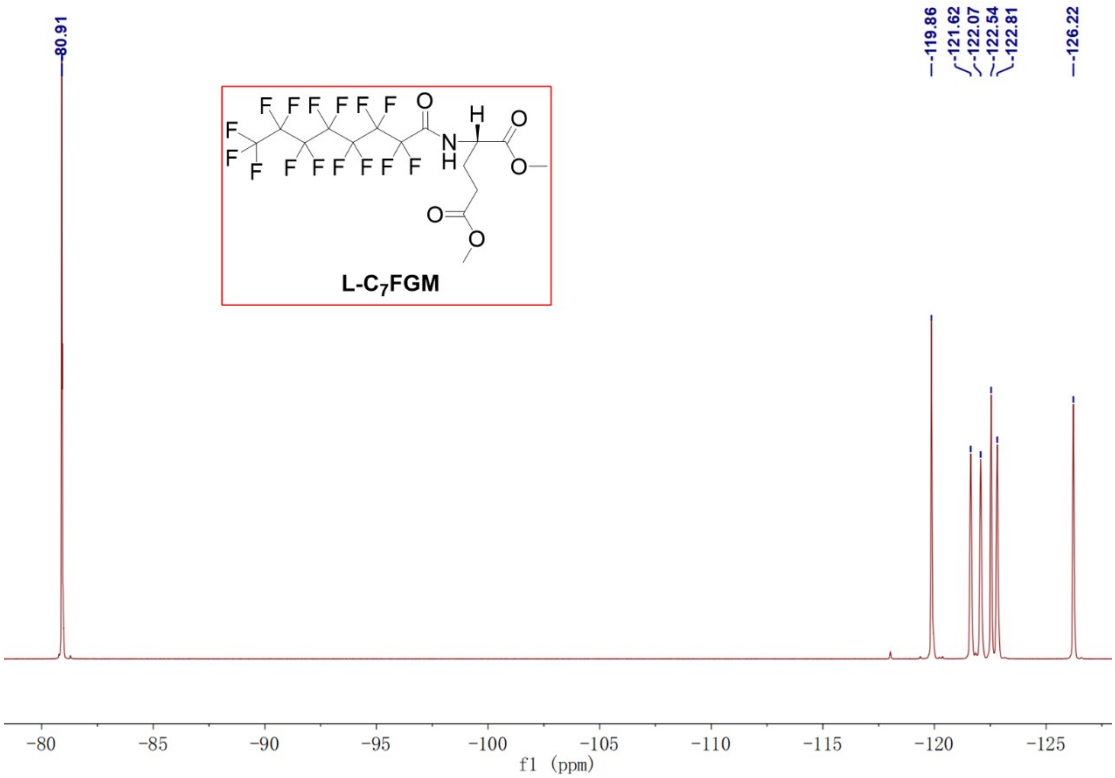

Figure S29 ^{19}F NMR spectrum of **L-C$_7$FGM.**

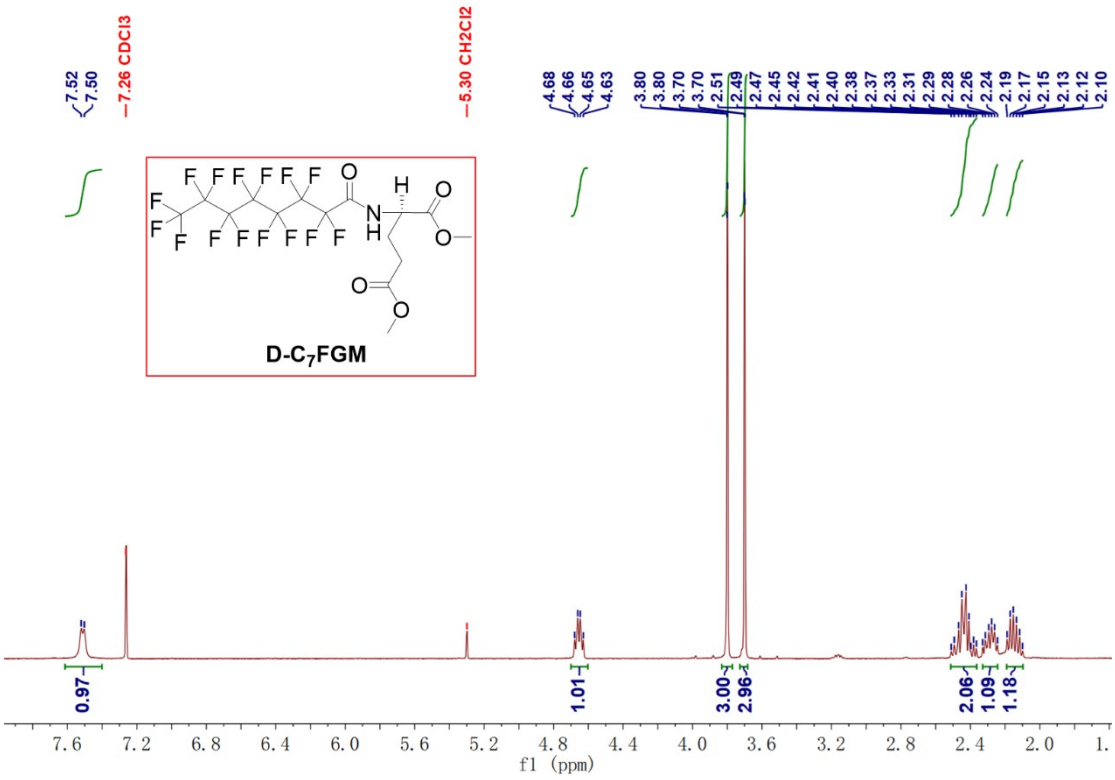

Figure S30 ^{1}H NMR spectrum of **D-C$_7$FGM**. The peak at 7.26 ppm is attributed to the solvent peak of Chloroform-d. The peak at 5.30 ppm is attributed to the residual solvent peak of CH_2Cl_2.

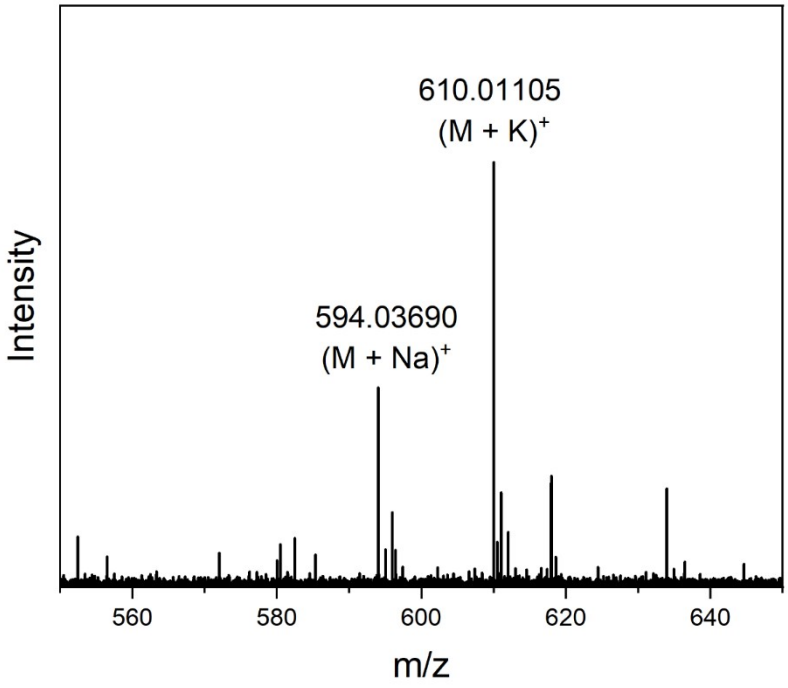

Figure S31 MALDI-FITCR-MS of **L-C$_7$FGM**. The two marked peaks represent the ion peaks of one **L-C$_7$FGM** combined with one sodium ion and one potassium ion respectively.

References

1. M. J. Abraham, T. Murtola, R. Schulz, S. Páll, J. C. Smith, B. Hess and E. Lindahl, *SoftwareX*, 2015, **1-2**, 19-25.
2. G. W. T. M.J. Frisch, H.B. Schlegel, G.E. Scuseria, M.A. Robb, J.R. Cheeseman, G. Scalmani, V. Barone, G.A. Petersson, H. Nakatsuji, X. Li, M. Caricato, A.V. Marenich, J. Bloino, B.G. Janesko, R. Gomperts, B. Mennucci, H.P. Hratchian, J.V. Ortiz, A.F. Izmaylov, J.L. Sonnenberg, D. Williams-Young, F. Ding, F. Lipparini, F. Egidi, J. Goings, B. Peng, A. Petrone, T. Henderson, D. Ranasinghe, V.G. Zakrzewski, J. Gao, N. Rega, G. Zheng, W. Liang, M. Hada, M. Ehara, K. Toyota, R. Fukuda, J. Hasegawa, M. Ishida, T. Nakajima, Y. Honda, O. Kitao, H. Nakai, T. Vreven, K. Throssell, J.A. Montgomery, J.E. Peralta, F. Ogliaro, M.J. Bearpark, J.J. Heyd, E.N. Brothers, K.N. Kudin, V.N. Staroverov, T.A. Keith, R. Kobayashi, J. Normand, K. Raghavachari, A.P. Rendell, J.C. Burant, S.S. Iyengar, J. Tomasi, M. Cossi, J.M. Millam, M. Klene, C. Adamo, R. Cammi, J.W. Ochterski, R.L. Martin, K. Morokuma, O. Farkas, J.B. Foresman and D.J. Fox, Gaussian, *Journal*, 2019.
3. A. D. Becke, *J. Chem. Phys.*, 1993, **98**, 5648-5652.
4. T. Lu and F. Chen, *J. Comput. Chem.*, 2012, **33**, 580-592.
5. T. Lu, *J. Chem. Phys.*, 2024, **161**, 082503.
6. T. Lu and Q. Chen, in *Conceptual Density Functional Theory*, 2022, DOI: https://doi.org/10.1002/9783527829941.ch31, pp. 631-647.
7. F. Neese, *WIREs Comput. Mol. Sci.*, 2022, **12**, e1606.